**Highlights**

- Explosion pressures, LFL, and UFL of alkene-containing mixtures in $N_2O$ are studied.
- $CH_4$, $C_2H_6$, n-$C_4H_{10}$, $C_2H_4$, and $C_3H_6$ are the alkenes tested in this study.
- Alkene–$N_2O$ mixtures exhibit higher explosion pressures than alkene–$O_2$ mixtures.
- LFLs for alkene-containing mixtures can be estimated using Le Chatelier's equation.
- A modified VAFT model can numerically estimate UFLs for alkene-containing mixtures.

# Numerical and experimental study of the explosion pressures and flammability limits of lower alkenes in nitrous oxide atmosphere

Yusuke Koshiba [a,] *, Takashi Hasegawa [b], Hideo Ohtani [c]

[a] Department of Materials Science and Chemical Engineering, Faculty of Engineering, Yokohama National University, 79-5 Tokiwadai, Hodogaya-ku, Yokohama 240-8501, Japan

[b] Graduate school of Environmental and Information Sciences, Yokohama National University, 79-7 Tokiwadai, Hodogaya-ku, Yokohama 240-8501, Japan

[c] Department of Safety Management, Faculty of Environmental and Information Sciences, Yokohama National University, 79-7 Tokiwadai, Hodogaya-ku, Yokohama 240-8501, Japan

* Corresponding author: Telephone number: +81 45 339 3985

Fax number: +81 45 339 3985

E-mail addresses: ykoshiba@ynu.ac.jp, koshiba-yusuke-xm@ynu.ac.jp

Postal address: 79-5 Tokiwadai, Hodogaya-ku, Yokohama 240-8501, Japan

1 The first two authors contributed equally to this work.

**Abstract**

This article reports an experimental and numerical investigation of the explosive properties of flammable mixtures of lower alkenes in nitrous oxide atmospheres. The motivation for this study was to reduce fire/explosion risks in industrial facilities that handle nitrous oxide. In this study, explosion pressures and lower and upper flammability limits were experimentally determined at an initial temperature of approximately 20 °C and an initial pressure of 101.3 kPa. The lower alkanes/alkenes methane, ethane, n-butane, ethylene, and propylene were tested. To precisely estimate the upper flammability limits of alkane–alkene–$N_2O$ and alkene–alkene–$N_2O$ mixtures, we proposed a modified VAFT (variable adiabatic flame temperature) method. Experimental measurements and numerical calculations clearly demonstrated that (i) alkene–$N_2O$ mixtures exhibit higher explosion pressures than the corresponding alkene–$O_2$ mixtures under fuel-lean conditions, (ii) Le Chatelier's equation successfully predicts the lower flammability limits of alkane–alkene–$N_2O$ and alkene–alkene–$N_2O$ mixtures, and (iii) the modified VAFT method can predict the upper flammability limits of alkane–alkene–$N_2O$ and alkene–alkene–$N_2O$ mixtures more accurately than Le Chatelier's equation.

**Keywords**: $N_2O$, Lower and upper flammability limits, Explosion pressure, Variable adiabatic flame temperature (VAFT), Olefin, Gas explosion

**Abbreviations**

| | |
|---|---|
| $a_1$–$a_6$ | coefficients in the thermodynamic equation |
| AFT | adiabatic flame temperature (K) |
| $C_p$ | heat capacity (J mol$^{-1}$ K$^{-1}$) |
| $C_{p,\,total}$ | total-product heat capacity (J mol$^{-1}$ K$^{-1}$) |
| $C_{st}$ | stoichiometric concentration of a fuel (vol%) |
| FL | flammability limit (vol%) |
| $H$ | enthalpy (J mol$^{-1}$) |
| $\Delta H_c$ | standard enthalpy of combustion (J mol$^{-1}$ or kJ mol$^{-1}$) |
| LFL | lower flammability limit (vol%) |
| $n$, $m$ | positive integer of fuels |
| $N_2O$ | nitrous oxide |
| $P_{ex}$ | observed explosion pressure (MPa) |
| $P_{cal}$ | theoretical explosion pressure (MPa) |
| $R$ | gas constant (J mol$^{-1}$ K$^{-1}$) |
| $T$ | temperature (K) |
| UFL, $U$ | upper flammability limit (vol%) |

| | |
|---|---|
| VAFT | variable adiabatic flame temperature (K) |
| $v_1$–$v_4$ | stoichiometric coefficients in the global reactions |
| $x_k$ | molar fraction of fuel component *k* (dimensionless) |
| $y_k$ | molar fraction of product species *k* (dimensionless) |

Greek letters

| | |
|---|---|
| $\varphi$ | equivalence ratio (dimensionless) |
| $\tau_{ex}$ | time to explosion pressure (ms) |
| $\chi$ | molar fraction of fuel (dimensionless) |

Superscripts

| | |
|---|---|
| ad | adiabatic |
| ° | standard |

Subscripts

| | |
|---|---|
| cal | calculated |
| *k* | chemical species, *k* |
| mix | mixture |

## 1. Introduction

Nitrous oxide ($N_2O$) exhibits affects global warming approximately 300 times more severely than carbon dioxide and is also an ozone-depleting anthropogenic substance (Ravishankara et al., 2009). Nitrous oxide, however, is a useful oxidant in industrial processes because (i) nitrous oxide is thermochemically stable under ambient conditions, (ii) nitrous oxide that contains 36% active oxygen by mass is an economical oxidizing agent (Newman et al., 2015), and (iii) the only significant byproduct of this oxidation reaction is $N_2$ gas. Hence, nitrous oxide has recently attracted increasing research attention; for instance, Branco et al. (2012) reported a method for converting methane ($CH_4$) over bimetallic catalysts using nitrous oxide as oxidizing agent. Poh et al. (1999) proposed an oxidation reaction of phosphines with nitrous oxide to avoid the use of flammable organic solvents, and Yamada et al. (2001) developed an olefin oxidation method that uses nitrous oxide and ruthenium complexes. Although such research is promising, several serious explosion accidents caused by nitrous oxide have been reported. For example, in the United States, a nitrous oxide trailer exploded, leading to one death (US Chemical Safety and Hazard Investigation Board, 2017), while in Japan, a gas cylinder explosion killed two people (Hirano, 2004).

Against such a background, gaining a clear insight into the explosive characteristics of

flammable mixtures is of great importance for both assessing fire and explosion risks and guaranteeing safety in chemical and process industries. Among the explosive characteristics of a mixture, knowing the flammability limits is important for preventing industrial accidents. However, despite the background described above, few papers have been hitherto published on the flammability limits of various fuels in nitrous oxide atmospheres, although flammability limits have frequently been studied in other atmospheres. Razus et al. (2017) studied the explosive properties of methane–$N_2O$ mixtures diluted with inert gases: He, $N_2$, Ar, and $CO_2$. Koshiba et al. (2015) measured the variation of flammability limits as a function of the carbon number of C1–C7 alkanes in $N_2O$. Vandebroek et al. (2005) examined the lower and upper flammability limits (LFL and UFL, respectively) of toluene–$N_2O$ mixtures at an initial temperature of 70 °C and atmospheric pressure (LFL = 0.25 vol% and UFL = 22.5 vol%). Unfortunately, only limited data on the flammability limits of alkene–$N_2O$ mixtures are available (Movileanu et al., 2015), let alone these of alkane–$N_2O$ mixtures.

The present study was designed with the following objectives in mind:

- To experimentally measure the explosion pressures ($P_{ex}$) and time to the explosion pressures ($\tau_{ex}$) of various alkene–$N_2O$ mixtures.
- To experimentally measure the flammability limits of alkene-containing mixtures:

alkane–alkene–$N_2O$ and alkene–alkene–$N_2O$ mixtures.

- To numerically estimate the flammability limits of alkane–alkene–$N_2O$ and alkene–alkene–$N_2O$ mixtures using Le Chatelier's and modified variable adiabatic flame temperature (VAFT) methods.

In this study, the following lower alkanes and lower alkenes were tested as fuels: $CH_4$, ethane ($C_2H_6$), n-butane (n-$C_4H_{10}$), ethylene ($C_2H_4$), and propylene ($C_3H_6$). The explosion pressures, times to the explosion pressures (Fig. 1), and flammability limits of the mixtures tested in this study were measured at an initial temperature of approximately 20 °C and an initial pressure of 101.3 kPa.

## 2. Experimental methods

### *2.1 Gases*

The present tests employed dry $CH_4$, $C_2H_6$, n-$C_4H_{10}$, $C_2H_4$, and $C_3H_6$ gases as fuels, and their purities were as follows: >99.999% ($CH_4$), >99.7% ($C_2H_6$), >99.95% (n-$C_4H_{10}$), >99.9% ($C_2H_4$), and >99.5% ($C_3H_6$). $N_2O$, $O_2$, and $N_2$ were >99.99% pure.

*2.2 Experimental apparatus*

The flammability limits were measured using the experimental apparatus illustrated in Fig. 2, which is the same as that used in an earlier study (Koshiba et al., 2010). The closed cylindrical chamber (100 mm in diameter and 120-mm high, i.e., 0.94 L) includes tungsten electrodes (1.0 mm in diameter) for ignition, a stirrer (1000 rpm), and two pressure transducers. The transducer (PTI-S, Swagelok, USA) placed on the top of the explosion chamber is used to monitor the partial pressures of the component gases, while the sensitive transducer (PGM-H, Kyowa Electronic Inst. Co., Ltd., Japan) located on the chamber side was used to measure the explosion pressure. The observed explosion pressures were recorded on a personal computer connected to the apparatus by a measuring unit (NR 500 and NR ST 04, Keyence Co., Japan).

*2.3 Experimental procedures*

The experimental procedures described here are the same as those of our earlier study (Koshiba et al., 2010). The explosion chamber was evacuated using a vacuum pump before each flammability limit test. The partial pressure method was employed to prepare gas mixtures in the chamber, and the mixtures were then mechanically mixed using the stirrer for at least one minute. At the quiescent

condition, an electric-spark discharge (18 J) between the electrodes was applied to ignite the center of the chamber; this spark was powered with a neon transformer.

In this study, the 7% pressure-rise criterion was applied and each test was repeated three times to confirm reproducibility. Each measurement was performed at an initial temperature of approximately 20 °C and initial pressure of 101.3 kPa.

## 3. Numerical calculation methods

### *3.1 Thermochemical equilibrium calculations*

If chemical reactions are allowed to reach equilibrium unimpeded and no heat loss is assumed, the adiabatic flame temperature (AFT), equilibrium composition, and theoretical explosion pressure ($P_{cal}$) can be computed by minimizing the Gibb's free energy (Melhem, 1997).

The CHEMKIN software package (v. 4.1.1, Kee et al., 2007) was used to compute the AFTs, equilibrium compositions of lower- and upper-limit mixtures, and adiabatic pressure (i.e., theoretical explosion pressures, $P_{cal}$). The following 34 chemical species were used in the calculations: C, CO, $CO_2$, CH, $CH_2$, $CH_3$, $CH_4$, $C_2$, $C_2H_2$, $C_2H_4$, $C_2H_5$, $C_2H_6$, $C_3$, $C_4$, $C_5$, $C_6H_6$, HCO, CN, H, $H_2$, OH, $HO_2$, $H_2O$, $H_2O_2$, O, $O_2$, N, $N_2$, NO, $NO_2$, $N_2O$, NH, HNO, and the fuels. The calculations postulated

that each gas behaves like an ideal gas.

### *3.2 Prediction of flammability limits*

#### *3.2.1 Literature review*

As described above, the flammability limit is a key index for ensuring safe operations. To date, several methods for estimating flammability limits are available in the literature. For instance, for unary fuel mixtures, Jones (1938) reported the following empirical equations (Eqs. (1) and (2)).

$$\boldsymbol{LFL = 0.55C_{st}}, \#(\mathbf{1})$$

$$\boldsymbol{UFL = 3.50C_{st}}, \#(\mathbf{2})$$

where $C_{st}$ is the stoichiometric concentration of a fuel. By using LFL and UFL data for typical organic compounds, excepting halogen-containing fuels, Suzuki (1994) and Suzuki & Koide (1994) developed the following empirical equations (Eqs. (3) and (4)).

$$\boldsymbol{LFL = -3.42\Delta H_c^{-1} + 0.569\Delta H_c + 0.0538\Delta H_c^2 + 1.80}, \#(\mathbf{3})$$

$$\boldsymbol{UFL = 6.30\Delta H_c + 0.567\Delta H_c^2 + 23.5}, \#(\mathbf{4})$$

where $\Delta H_c$ is the standard enthalpy of combustion in units of J mol$^{-1}$.

For binary fuel mixtures, Le Chatelier's formula (Eq. (5)) is the most well-known method for estimating flammability limits (Drysdale, 2011).

$$\boldsymbol{FL_{mix} = \frac{1}{\sum \frac{x_k}{FL_k}}}, \#(\mathbf{5})$$

where $FL_{mix}$ is the flammability limit of a mixture, $x_k$ is the mole fraction of component $k$ such that $\sum x_k = 100$ vol%, and $FL_k$ is the flammability limit for fuel $k$. Several studies have been published about the applicability of Le Chatelier's rule to binary fuel mixtures. For instance, Zhao et al. (2009) demonstrated that, for lower-limit binary hydrocarbon–air mixtures, the values calculated from Le Chatelier's equation fit well with the corresponding experimental LFL values, while for upper-limit binary hydrocarbon–air mixtures, Le Chatelier's equation must be empirically modified by powering the hydrocarbon concentrations. For upper-limit fuel–air mixtures, Kondo et al. (2008) extended Le Chatelier's equations by manipulating the fitting parameter.

For alkene-containing mixtures, several researchers have developed methods for estimating

flammability limits using AFTs. Vidal et al. (2006) demonstrated that, for ethylene–air–$N_2$ mixtures, computed LFL values agreed well with corresponding experimental values when the calculations are performed with a fixed AFT of 1400 K. Zhao et al. (2010) developed a method for estimating LFLs for alkane–alkene–air and alkene–alkene–air mixtures using average flame temperatures. Liaw et al. (2012) presented a model to estimate the LFLs of $N_2$-diluted ethylene–air and propylene–air mixtures using constant flame temperatures. A prediction method for UFLs of binary hydrocarbon–air mixtures using calculated AFTs was developed by Mendiburu et al. (2016). However, in general, UFLs are difficult to estimate precisely; in addition, no methods for estimating the UFLs of specifically $N_2O$-containing mixtures are found in the literature.

### *3.2.2 Predicting UFL using the modified VAFT method*

Recently, Wu et al. (2018) reported a new prediction method for the UFLs of alkane–air mixtures diluted with $CO_2$ based on the VAFT method, which semi-empirically estimates the UFL values. According to Wu et al., the VAFT model employed several assumptions that (i) the pressure remains constant during the combustion process, (ii) the AFT is positively correlated with the concentration of the diluent (i.e., $CO_2$), and (iii) the main combustion products at the UFL are carbon monoxide (CO), $CO_2$, $H_2O$, $H_2$, and $N_2$.

Later in this article, a modified VAFT model to estimate the UFLs for alkane–alkene–$N_2O$ and

alkene–alkene–$N_2O$ mixtures is proposed. As noted later in Section 4.4, when lower alkanes and alkenes are used as fuel, the mole fractions of $H_2O$ are quite low (~$10^{-5}$) at the UFLs of alkane–alkene–$N_2O$ and alkene–alkene–$N_2O$ mixtures, whereas the mole fraction of acetylene ($C_2H_2$) is high (~$10^{-4}$–$10^{-2}$). Hence, in this study, we made the following assumptions so that the UFL values could be calculated: (i) combustion processes occur at a constant pressure, (ii) AFT varies with the fuel mole fraction, and (iii) the major chemical species at the upper-limit mixtures examined in this study are CO, $H_2$, "$C_2H_2$," and $N_2$. For alkane–alkene–$N_2O$ mixtures, the modified VAFT model assumes the following global reaction scheme (Eq. (6)):

$$\boldsymbol{\chi U C_n H_{2n+2} + (1-\chi) U C_m H_{2m} + (1-U) N_2O \rightarrow v_1 CO + v_2 H_2 + v_3 C_2 H_2 + v_4 N_2 + \Delta H_{c,1} \#(6)}$$

where $U$ is the UFL of the fuel, $v_1$–$v_4$ are the stoichiometric coefficients in the global reaction, $\Delta H_{c,1}$ is the enthalpy of combustion for the reaction, and $\chi$ denotes the mole fraction of $C_nH_{2n+2}$ in the fuels.

The complete combustion reaction for each component gas in Eq. (6) is as follows (Eqs. (7)–(10)):

$$\boldsymbol{C_n H_{2n+2} + (3n+1) N_2O \rightarrow n CO_2 + (n+1) H_2O + (3n+1) N_2 + \Delta H_{C,C_n H_{2n+2}} \#(7)}$$

$$\mathbf{CO + N_2O \rightarrow CO_2 + N_2 + \Delta H_{C,CO}\#(8)}$$

$$\mathbf{H_2 + N_2O \rightarrow H_2O + N_2 + \Delta H_{C,H_2}\#(9)}$$

$$\mathbf{C_2H_2 + 5N_2O \rightarrow 2CO_2 + H_2O + 5N_2 + \Delta H_{C,C_2H_2}\#(10)}$$

Substituting Eqs. (7)–(10) into Eq. (6) yields Eq. (11):

$$\boldsymbol{\Delta H_{C,1} = \chi U \Delta H_{C,C_nH_{2n+2}} + (1-\chi) U \Delta H_{C,C_mH_m} - v_1 \Delta H_{C,CO} - v_2 \Delta H_{C,H_2} - v_3 \Delta H_{C,C_2H_2}\#(11)}$$

Using the mass conservation law, the following Eqs. (12)–(15)) result.

$$\boldsymbol{v_1 + 2v_2 = n\chi U + m(1-\chi)U\#(12)}$$

$$\boldsymbol{v_1 = 1 - U\#(13)}$$

$$\boldsymbol{v_2 + v_3 = (n+1)\chi U + m(1-\chi)U\#(14)}$$

$$\boldsymbol{v_4 = 1 - U}. \#(\mathbf{15})$$

On the basis of the law of conservation of energy, Eq. (16) results:

$$\boldsymbol{v_1 H^{\circ}_{CO} + v_2 H^{\circ}_{H_2} + v_3 H^{\circ}_{C_2H_2} + v_4 H^{\circ}_{N_2} + \Delta H_{c,1} = v_1 H^{ad}_{CO} + v_2 H^{ad}_{H_2} + v_3 H^{ad}_{C_2H_2} + v_4 H^{ad}_{N_2}} \#(\mathbf{16})$$

where $H_k^{\circ}$ and $H_k^{ad}$ represent the enthalpy of species $k$ at 298 K and the AFT, respectively. The enthalpy of species $k$ is calculated using Eq. (17).

$$\boldsymbol{\frac{H}{RT} = a_1 + \frac{a_2}{2}T + \frac{a_3}{3}T^2 + \frac{a_4}{4}T^3 + \frac{a_5}{5}T^4 + \frac{a_6}{T}} \#(\mathbf{17})$$

where $a_1$–$a_6$ are the thermodynamic coefficients of each species $k$, and these were extracted from a thermodynamic database (NASA, 2001). $R$ and $T$ represent the gas constant and temperature, respectively. The UFLs, $U$, were calculated by solving Eq. (16) using Eqs. (11)–(15) and (17).

Like the alkane–alkene–$N_2O$ mixtures, $U$ values for alkene–alkene–$N_2O$ mixtures were numerically computed on the basis of the following global reaction (Eq. (18)):

$$\chi U\mathbf{C}_n\mathbf{H}_{2n} + (1-\chi)U\mathbf{C}_m\mathbf{H}_{2m} + (1-U)\mathbf{N}_2\mathbf{O} \rightarrow v_1\mathbf{CO} + v_2\mathbf{H}_2 + v_3\mathbf{C}_2\mathbf{H}_2 + v_4\mathbf{N}_2 + \Delta H_{c,2} \# (18)$$

where $\Delta H_{c,2}$ is the enthalpy of combustion for the reaction.

## 4. Results and discussion

### *4.1 Explosion pressures and times to explosion pressures of alkene–$N_2O$ mixtures diluted with $N_2$*

Owing to their high explosion pressures, each mixture tested was diluted with 30 vol% $N_2$ so that the experiments were safe for researchers in the lab. The mixture composition in our tests was 70 vol% of alkene–$N_2O$ and 30 vol% of $N_2$.

Fig. 3a and 3b plots the explosion pressures and times to the corresponding explosion pressures of $C_2H_4$–$N_2O$–$N_2$ and $C_3H_6$–$N_2O$–$N_2$ mixtures, respectively, as a function of the equivalence ratio, $\varphi$, varying from $\varphi = 0.4$ to $\varphi = 2.4$. For reference, the corresponding graphs for $O_2$-containing mixtures (i.e., $C_2H_4$–$O_2$–$N_2$ and $C_3H_6$–$O_2$–$N_2$ mixtures) are plotted in Fig. 4a and 4b, respectively. The explosion pressure for the $C_2H_4$–$N_2O$–30 vol% $N_2$ mixture in the 0.94-L vessel was determined to be $P_{ex} = 1.44$ MPa when $\varphi = 1.0$. As expected, the values we observed were higher than those of approximately of a stoichiometric $C_2H_4$–$N_2O$–60 vol% $N_2$ mixture in a 1.18-L vessel, $P_{ex} = 0.7$ MPa,

reported by Movileanu et al. (2015).

For both the $C_2H_4$–$O_2$–$N_2$ and the $C_3H_6$–$O_2$–$N_2$ mixtures, the explosion pressures exhibited a similar inverted U-shaped curve, and the time to the corresponding explosion pressure showed the same trend. Comparison of Fig. 3 with Fig. 4 indicates that the alkene–$N_2O$–$N_2$ mixtures exhibited the higher explosion pressures than the corresponding alkene–$O_2$–$N_2$ mixtures under fuel-lean conditions. Comparison of Fig. 3 with Fig. 4 reveals that the $\varphi$ values for the $N_2O$ mixtures at which the maximum explosion pressure is observed are smaller than those for the corresponding $O_2$ mixtures ($C_2H_4$–$N_2O$–$N_2$: $\varphi = 1.4$, $C_2H_4$–$O_2$–$N_2$: $\varphi = 1.8$; $C_3H_6$–$N_2O$–$N_2$: $\varphi = 1.6$, $C_3H_6$–$O_2$–$N_2$: $\varphi = 1.8$). This difference is probably explained by the decomposition reaction of $N_2O$. Unlike $O_2$, nitrous oxide readily decomposes during combustion, according to Eq. (19) (Parres-Esclapez et al., 2010), which significantly enhances the observed explosion pressure. In fact, equilibrium calculations verified that the mole fraction of $N_2O$ was less than $10^{-6}$. The initial mole fraction of $N_2O$ decreases as the $\varphi$ value increases, accordingly lowering the explosion pressure caused by $N_2O$ decomposition. A similar trend is reported in the literature (Koshiba et al., 2015).

$$\mathbf{N_2O \rightarrow N_2 + \frac{1}{2}O_2 \#(19)}$$

The theoretical explosion pressures are also presented in Figs. 3 and 4. In general, as also pointed

out by Salzano et al (2012), the experimentally observed explosion pressure is significantly lower than the corresponding calculated explosion pressure. This difference is accounted for by heat losses at the vessel walls. However, interestingly, no significant differences were found in terms of explosion pressure between the experimental and calculated values for the $C_2H_4$–$O_2$–$N_2$ and $C_3H_6$–$O_2$–$N_2$ mixtures. This may imply that the heat loss at the wall surface is negligible when combusting these mixtures.

### *4.2 Flammability limits of $C_2H_4$–$N_2O$ and $C_3H_6$–$N_2O$ mixtures*

Table 1 lists the LFLs and UFLs of the $C_2H_4$–$N_2O$ and $C_3H_6$–$N_2O$ mixtures, together with $C_2H_4$–$O_2$, $C_3H_6$–$O_2$, $C_2H_4$–air, and $C_3H_6$–air mixtures for reference. As shown in this table, the flammable range of $C_2H_4$–$N_2O$ was determined to be 2.0–40.0 vol%, while that of $C_3H_6$–$N_2O$ was 1.5–28.7 vol%.

For the same alkene, the mixtures are ranked in terms of their LFLs as follows: alkene/air ≈ alkene/$O_2$ > alkene/$N_2O$; this ordering is in good agreement with that for alkane mixtures (alkane/air ≈ alkane/$O_2$ > alkane/$N_2O$, Koshiba et al., 2015). This implies that a fuel in an $N_2O$ atmosphere more readily creates a flammable mixture than a fuel in air or $O_2$ atmospheres.

### *4.3 LFLs of alkane–alkene–$N_2O$ and alkene–alkene–$N_2O$ mixtures*

The LFLs of alkane–alkene–$N_2O$ and alkene–alkene–$N_2O$ mixtures are discussed in this section. As an example, Fig. 5a–5c shows the variations of the LFLs as a function of $x_{\text{fuel-1}}$ ($x_{\text{ethylene}}$ or $x_{\text{methane}}$) for the $C_2H_4$–*n*-$C_4H_{10}$–$N_2O$, $CH_4$–$C_3H_6$–$N_2O$, and $C_2H_4$–$C_3H_6$–$N_2O$ mixtures, respectively. Fig. 5 also plots the curves calculated from Eq. (5) for these lower-limit mixtures. As seen in the figure, the maximum absolute differences between the observed LFLs and the calculated curves are 0.1 vol%, which is within experimental error.

As stated by Crowl and Louvar (2011a), Le Chatelier's rule relies upon the following basic assumptions: (i) the total heat capacity of reaction products is constant, (ii) the combustion kinetics of the pure species is independent and unchanged, and (iii) AFT is independent of fuel fraction. The total-product heat capacity is calculated with the following equation (Eq. (20)):

$$\boldsymbol{C_{\mathrm{p,total}} = \sum C_{\mathrm{p},k} \cdot y_k \#(20)}$$

where $C_{\text{p, total}}$, $C_{\text{p, }k}$, and $y_{k,}$ denote the total-product heat capacity, heat capacity of product species *k*, and mole fraction of product species *k*, respectively.

In Fig. 6a, the total-product heat capacities calculated from Eq. (20) and AFTs for the lower-limit

$C_2H_4$–*n*-$C_4H_{10}$–$N_2O$ mixture are plotted as a function of $x_{ethylene}$ in the fuels. Fig. 6b shows the equilibrium compositions of the main species with mole fraction greater than $10^{-2}$ for the lower-limit $C_2H_4$–*n*-$C_4H_{10}$–$N_2O$ mixture. As seen in Fig. 6, the three parameters (i.e., total-product heat capacity, equilibrium composition, and AFT) remained unchanged for various values of *x*. The results in Figs 7 and 8 also confirm similar trends for the $CH_4$–$C_3H_6$–$N_2O$ and $C_2H_4$–$C_3H_6$–$N_2O$ mixtures. Hence, as with lower-limit alkane–alkane–$N_2O$ mixtures (Koshiba et al., 2017), we concluded that Le Chatelier's rule holds for the lower-limit alkane–alkene–$N_2O$ and alkene–alkene–$N_2O$ mixtures examined in this study.

### *4.4 UFLs of alkane–alkene–$N_2O$ and alkene–alkene–$N_2O$ mixtures*

The UFLs of $CH_4$–$C_3H_6$–$N_2O$, $C_2H_4$–$C_2H_6$–$N_2O$, and $C_2H_4$–$C_3H_6$–$N_2O$ mixtures are plotted as a function of $x_{fuel\text{-}1}$ (i.e., $x_{ethylene}$ or $x_{methane}$) in Fig. 9a–9c, respectively. For the alkane–alkene–$N_2O$ and alkene–alkene–$N_2O$ mixtures, the UFLs exhibited flattened S-shaped or inverted S-shaped curves. Note that the curve shape (i.e., S-shaped or inverted S-shaped) varies depending on the combination of fuels tested. Similar behavior was also reported by Zhao et al. (2009), who studied the UFLs of methane–ethylene–air and ethylene–propylene–air mixtures.

Unlike the lower-limit alkane–alkene–$N_2O$ and alkene–alkene–$N_2O$ mixtures discussed in

Section 4.3, the upper-limit alkane–alkene–$N_2O$ and alkene–alkene–$N_2O$ mixtures tested in this study did not satisfy the assumptions involved in Le Chatelier's equation (data not shown). As also depicted in Fig. 9, the $CH_4$–$C_3H_6$–$N_2O$, $C_2H_4$–$C_2H_6$–$N_2O$, and $C_2H_4$–$C_3H_6$–$N_2O$ mixtures showed relatively large differences between the observed UFLs and the curves calculated from Eq. (5). Hence, Le Chatelier's equation is not accurate for these mixtures. Such result is consistent with the finding of Zhao et al. (2009) that Le Chatelier's equation cannot always precisely predict UFL values for mixtures that contain alkenes.

As an example, the relation between the species mole fractions ($>10^{-4}$) and $x_{\mathrm{ethylene}}$ for the upper-limit $C_2H_4$–$C_2H_6$–$N_2O$ mixture is shown in Fig. 10. The major species are clearly $H_2$, $N_2$, CO, and $C_2H_2$. In Figs. 9a–9c, UFL curves calculated using the modified VAFT method are also plotted for the $CH_4$–$C_3H_6$–$N_2O$, $C_2H_4$–$C_2H_6$–$N_2O$, and $C_2H_4$–$C_3H_6$–$N_2O$ mixtures, respectively. As the agreement of these latter curves with the experimental data shows, we therefore conclude that the VAFT method accurately estimates UFLs for lower alkane–alkene–$N_2O$ and lower alkene–alkene–$N_2O$ mixtures.

In summary, the modified VAFT model suggested in this study permits us to accurately estimate the flammability limits of alkane–alkene–$N_2O$ and lower alkene–alkene–$N_2O$ mixtures. However, note that the modified VAFT method includes an inherent limitation. In general, at UFLs, the insufficient amount of oxidant leads to incomplete combustion, resulting in the formation of soot. As

reported by Torrade et al. (2017) who investigated the explosion characteristics of hybrid mixtures (i.e., methane–air–nanosized-carbon black), explosion properties are generally influenced by the presence of soot. To obtain a closer estimate of UFLs, a new model that considers soot formation should be developed in future research.

## 5. Conclusions

In this study, the explosion pressures, times to the corresponding explosion pressures, and LFL and UFL of mixtures with lower alkenes (i.e., $C_2H_4$ and $C_3H_6$) in nitrous oxide atmospheres were measured experimentally at an initial temperature of ca. 20 °C and an initial pressure of 101.3 kPa. In addition, the LFL and UFL of alkane–alkene–$N_2O$ and alkene–alkene–$N_2O$ mixtures were numerically calculated using both Le Chatelier's equation and the modified VAFT method.

We draw the following conclusions from the experimental and numerical results.

(i) Under fuel-lean conditions, alkene–$N_2O$–$N_2$ mixtures exhibited higher explosion pressures than did corresponding alkene–$O_2$–$N_2$ mixtures.

(ii) For lower-limit alkane–alkene–$N_2O$ and alkene–alkene–$N_2O$ mixtures, the curves calculated from Eq. (5) agreed well with the experimental LFL data, implying that Le Chatelier's rule holds

for these lower-limit mixtures in nitrous oxide atmosphere.

(iii) For upper-limit alkane–alkene–$N_2O$ and alkene–alkene–$N_2O$ mixtures, Le Chatelier's equation does not agree with experimental UFL values. The modified VAFT method suggested in this study estimates the UFLs of these mixtures more accurately than Le Chatelier's equation.

This experimental and numerical study opens the way for estimating the LFL and UFL of lower alkane–alkene–$N_2O$ and alkene–alkene–$N_2O$ mixtures. The methods presented above will contribute to safety enhancement in industrial facilities that handle and store nitrous oxide.

**Conflict of interest**

The authors declare that there are no conflicts of interest.

**References**

Branco, J.B., Ferreira, A.C., Botelho do Rego, A.M., Ferraria, A.M., Almeida-Gasche, T., 2012. Conversion of methane over bimetallic copper and nickel actinide oxides (Th, U) using nitrous oxide as oxidant. ACS Catal. 2, 2482–2489.

Chen, C.-C., 2011. A study on estimating flammability limits in oxygen. Ind. Eng. Chem. Res. 50, 10283–10291.

Crowl, D.A., Louvar, J.F., 2011a. Chemical Process Safety: Fundamentals with Applications, third ed. Pearson Education, Inc, Boston, pp. 253–254.

Crowl, D.A., Louvar, J.F., 2011b. Chemical Process Safety: Fundamentals with Applications, third ed. Pearson Education, Inc, Boston, pp. 688–689.

Crowl, D.A., Louvar, J.F., 2011c. Chemical Process Safety: Fundamentals with Applications, third ed. Pearson Education, Inc, Boston, p. 259.

Drysdale, D., 2011. An Introduction to Fire Dynamics, third ed. John Wiley & Sons. Ltd., West Sussex.

Hirano, T., 2004. Accidental explosions of semiconductor manufacturing gases in Japan. J. Loss Prev. Process Ind. 17, 29–34.

Jones, G.W., 1938. Inflammation limits and their practical application in hazardous industrial operations. Chem. Res. 22, 1–26.

Kee, R.J., Rupley, F.M., Miller, J.A., Coltrin, M.E., Grcar, J.F., Meeks, E., Mof-fat, H.K., Lutz, A.E., Dixon-Lewis, G., Smooke, M.D., Warnatz, J., Evans, G.H., Larson, R.S., Mitchell, R.E., Petzold, L.R., Reynolds W.C., Caracotsios, M., Stew-art, W.E., Glarborg, P., Wang, C., McLellan, C.L., Adigun, O., Houf, W.G., Chou, C.P., Miller, S.F., Ho, P., Young, P.D., Young, D.J., Hodgson, D.W., Petrova, M.V., Puduppakkam, K.V., 2007. CHEMKIN Release 4.1.1, Reaction Design, San Diego, CA.

Kondo, S., Takizawa, K., Takahashi, A., Tokuhashi, K., Sekiya, A., 2008. A study on flammability limits of fuel mixtures. J. Hazard. Mater. 155, 440–448.

Koshiba, Y., Hasegawa, T., Kim, B., Ohtani, H., 2017. Flammability limits, explosion pressures, and applicability of Le Chatelier's rule to binary alkane–nitrous oxide mixtures. J. Loss Prev. Process Ind. 45, 1–8.

Koshiba, Y., Nishida, T., Morita, N., Ohtani, H., 2015. Explosion behavior of n-alkane/nitrous oxide

mixtures. Process Saf. Env. Prot. 98, 11–15.

Koshiba, Y., Takigawa, T., Matsuoka, Y., Ohtani, H., 2010. Explosion characteristics of flammable organic vapors in nitrous oxide atmosphere. J. Hazard. Mater. 183, 746–753.

Liaw, H.-J., Chen, C.-C., Chang, C.-H., Lin, N.-K., Shu, C.-M., 2012. Model to estimate the flammability limits of fuel-air-diluent mixtures tested in a constant pressure vessel. Ind. Eng. Chem. Res. 51, 2747–2761.

Melhem, G.A., 1997. A detailed method for estimating mixture flammability limits using chemical equilibrium. Process Saf. Prog. 16, 203–218.

Mendiburu, A.Z., de Carvalho Jr., J.A., Coronado, C.R., 2016. Estimation of upper flammability limits of C–H compounds in air at standard atmospheric pressure and evaluation of temperature dependence. J. Hazard. Mater. 304, 512–521.

Movileanu, C., Razus, D., Mitu, M., Giurcan, V., Oancea, D., 2015. Explosion of $C_2H_4$–$N_2O$–$N_2$ in elongated closed vessels. in: Proc. 7th Eur. Combust. Meeting (P4-04).

NASA, 2001. Thermo Build. https://www.grc.nasa.gov/www/CEAWeb/ceaThermoBuild.htm (accessed 1 April 2018).

Newman, S.G., Lee, K., Cai, J., Yang, L., Green, W.H., Jensen, K.F., 2015. Continuous thermal oxidation of alkenes with nitrous oxide in a packed bed reactor. Ind. Eng. Chem. Res. 54, 4166–4173.

Parres-Esclapez, S., Illán-Gómez, M.J., Salinas-Martínez de Lecea,C., Bueno-López, A., 2010. On the importance of the catalystredox properties in the $N_2O$ decomposition over alumina andceria supported Rh, Pd and Pt. Appl. Catal. B: Environ. 96, 370–378.

Poh, S., Hernandez, R., Inagaki, M., Jessop, P.G., 1999. Oxidation of phosphines by surpercritical nitrous oxide. Org. Lett. 1, 583–585.

Ravishankara, A.R., Daniel, J.S., Portmann, R.W., 2009. Nitrous oxide ($N_2O$): the dominant ozone-depleting substance emitted in the 21st century. Science 326, 123–125.

Razus, D., Mitu, M., Giurcan, V., Oancea, D., 2017. Propagation indices of methane-nitrous oxide flames in the presence of inert additives. J. Loss Prev. Process Ind. 49, 418–426.

Salzano, E., Cammarota, F., Di Benedetto, A., Di Sarli, V., 2012. Explosion behavior of hydrogen-methane/air mixtures. J. Loss Prev. Process Ind. 25, 443–447.

Schröder, V., Molnarne, M., 2005. Flammability of gas mixtures Part 1: Fire potential. J. Hazard. Mater. A121, 37–44.

Suzuki, T., 1994. Empirical relationship between lower flammability limits and standard enthalpies of combustion of organic compounds. Fire Mater. 18, 333–336.

Suzuki, T., Koide, K., 1994. Correlation between upper flammability limits and thermochemical properties of organic compounds. Fire Mater. 18, 393–397.

Torrado, D., Buitrago, V., Glaude, P.-A., Dufaud, O., 2017. Explosions of methane/air/nanoparticles mixtures: comparison between carbon black and inert particles. Process Saf. Env. Prot. 110, 77–88.

US Chemical Safety and Hazard Investigation Board, 2017. Nitrous Oxide Explosion. Investigation report (#2016-04-I-FL).

Vandebroek, L., Van den Schoor, F., Verplaetsen, F., Berghmans, J., Winter, H., van't Oost, E., 2005. Flammability limits and explosion characteristics of toluene–nitrous oxide mixtures. J. Hazard. Mater. A120, 57–65.

Vidal, M., Wong, W., Rogers, W.J., Mannan, M.S., 2006. Evaluation of lower flammability limits of fuel–air–diluent mixtures using calculated adiabatic flame temperatures. J. Hazard. Mater. 130, 21–27.

Wu, M., Shu, G., Chen, R., Tian, H., Wang, X., Wang, Y., 2018. A new model based on adiabatic flame temperature for evacuation of the upper flammable limit of alkane–air–$CO_2$ mixtures. J. Hazard. Mater. 344, 450–457.

Yamada, T., Hashimoto, K., Kitaichi, Y., Suzuki, K., Ikeno, T., 2001. Nitrous oxide oxidation of olefins catalyzed by ruthenium porphyrin complexes. Chem. Lett. 30, 268–269.

Zhao, F., Rogers, W.J., Mannan, M.S., 2010. Calculated flame temperature (CFT) modeling of fuel mixture lower flammability limits. J. Hazard. Mater. 174, 416–423.

Zhao, F., Rogers, W.J., Mannan, M.S., 2009. Experimental measurement and numerical analysis of binary hydrocarbon mixture flammability limits. Process Saf. Env. Prot. 87, 94–104.

**Table caption**

Table 1

Lower and upper flammability limits of $C_2H_4$–$N_2O$ and $C_3H_6$–$N_2O$ mixtures, listed alongside previously reported values for $C_2H_4$–$O_2$, $C_3H_6$–$O_2$, $C_2H_4$–air, and $C_3H_6$–air mixtures.

**Figure captions**

Figure 1

Typical explosion pressure history in this study.

Figure 2

Experimental apparatus for explosion tests.

Figure 3

Observed explosion pressures (○, $P_{ex}$), theoretical explosion pressures (●, $P_{cal}$), and times to the corresponding explosion pressures (□, $\tau_{ex}$) as a function of the equivalence ratio, $\varphi$. (a) $C_2H_4$–$N_2O$ mixtures diluted with 30 vol% $N_2$ and (b) $C_3H_6$–$N_2O$ mixtures diluted with 30 vol% $N_2$.

Figure 4

Observed explosion pressures (○, $P_{ex}$), computed theoretical explosion pressures (●, $P_{cal}$), and times to the corresponding explosion pressures (□, $\tau_{ex}$) as a function of the equivalence ratio, $\varphi$. (a) $C_2H_4$–$O_2$ mixtures diluted with 30 vol% $N_2$ and (b) $C_3H_6$–$O_2$ mixtures diluted with 30 vol% $N_2$.

Figure 5

Lower flammability limits of (a) $C_2H_4$–*n*-$C_4H_{10}$–$N_2O$, (b) $CH_4$–$C_3H_6$–$N_2O$, and (c) $C_2H_4$–$C_3H_6$–$N_2O$ mixtures. The dashed curves are calculated from Eq. (5).

Figure 6

(a) Total-product heat capacity calculated from Eq. (20) and AFTs. (b) Equilibrium compositions for the lower-limit $C_2H_4$–*n*-$C_4H_{10}$–$N_2O$ mixtures.

Figure 7

(a) Total-product heat capacity calculated from Eq. (20) and AFTs. (b) Equilibrium compositions for the lower-limit $CH_4$–$C_3H_6$–$N_2O$ mixtures.

Figure 8

(a) Total-product heat capacity calculated from Eq. (20) and AFTs. (b) Equilibrium compositions for the lower-limit $C_2H_4$–$C_3H_6$–$N_2O$ mixtures.

Figure 9

UFLs of (a) $CH_4$–$C_3H_6$–$N_2O$, (b) $C_2H_4$–$C_2H_6$–$N_2O$, and (c) $C_2H_4$–$C_3H_6$–$N_2O$ mixtures. The dashed curves are computed from Eq. (5), and solid curves are calculated on the basis of the modified VAFT method.

Figure 10

Calculated equilibrium compositions for upper-limit $C_2H_4$–$C_3H_6$–$N_2O$ mixtures. Only the major species (mole fractions: $>10^{-4}$) are presented.

**Figure 1**

Figure 1

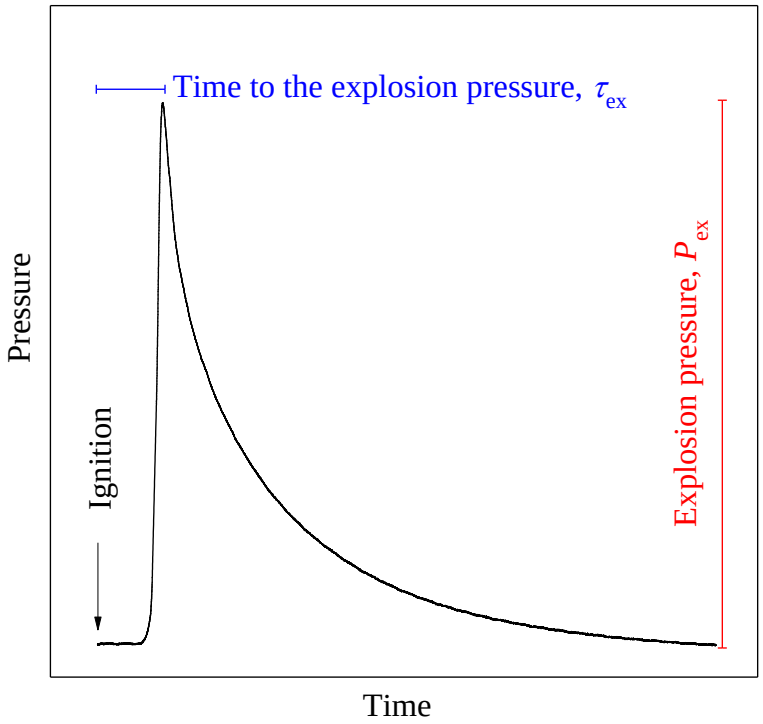

**Figure 2**

Figure 2

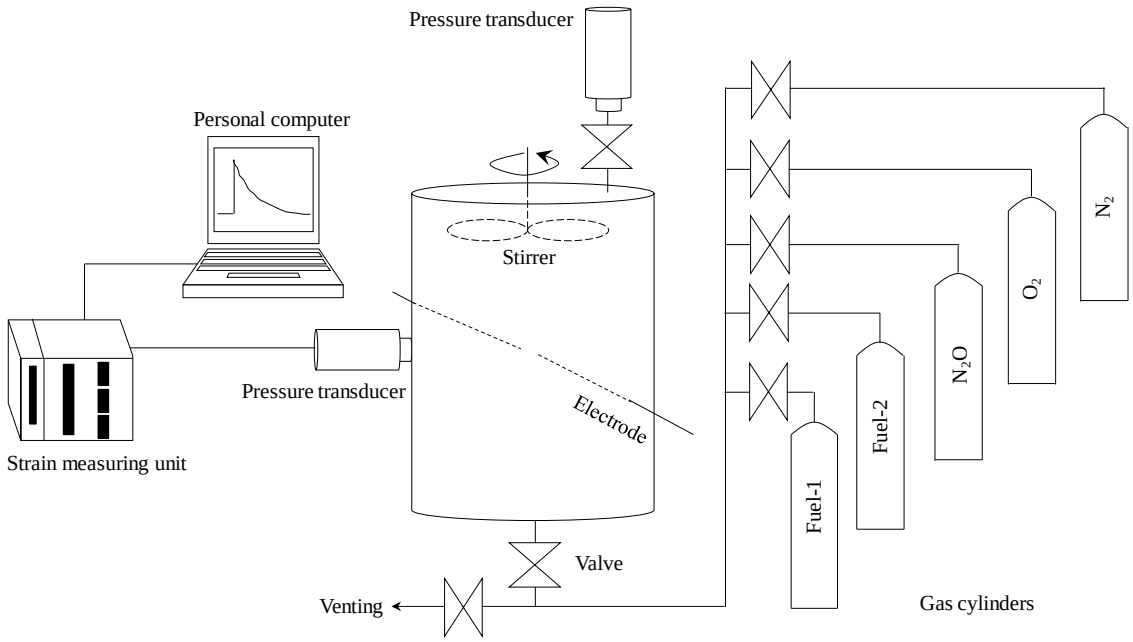

**Figure 3**

Figure 3

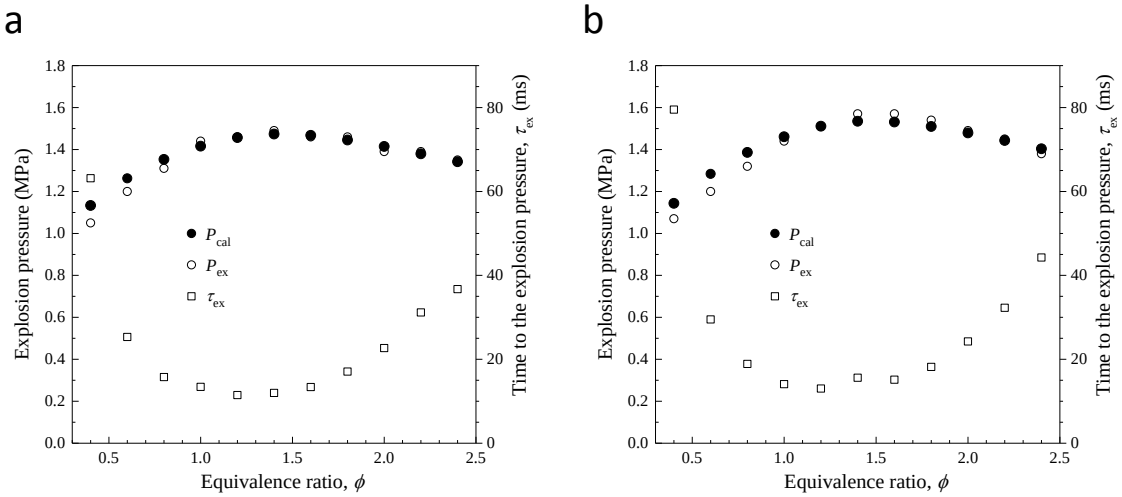

**Figure 4**

Figure 4

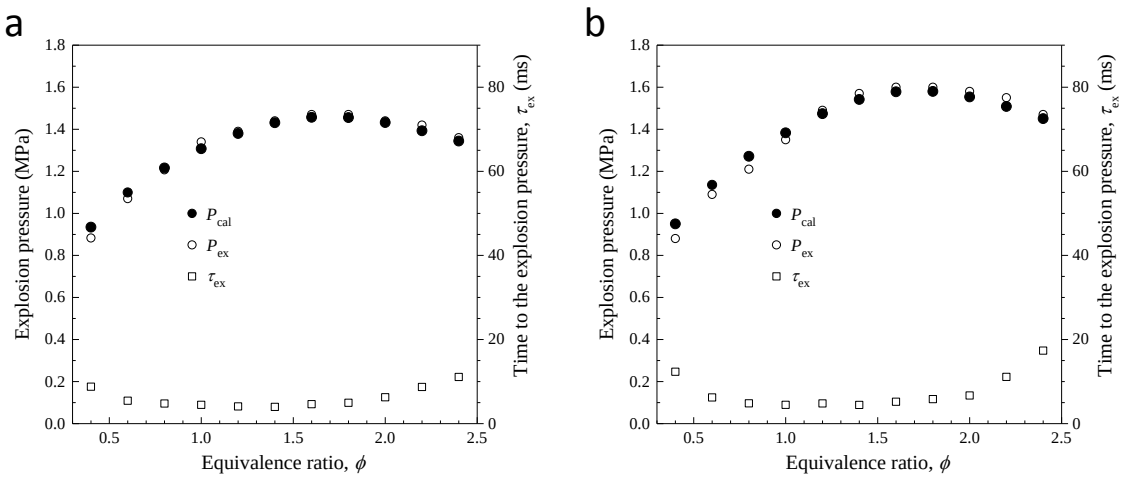

**Figure 5**

Figure 5

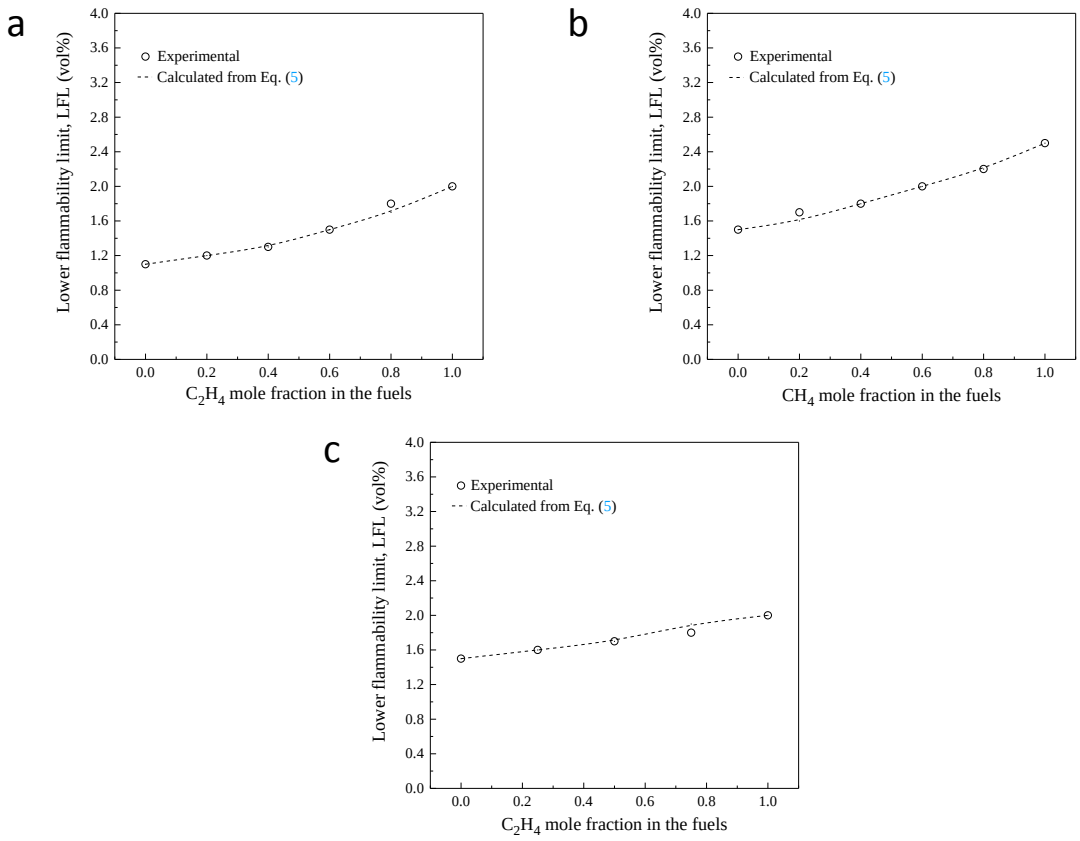

**Figure 6**

Figure 6

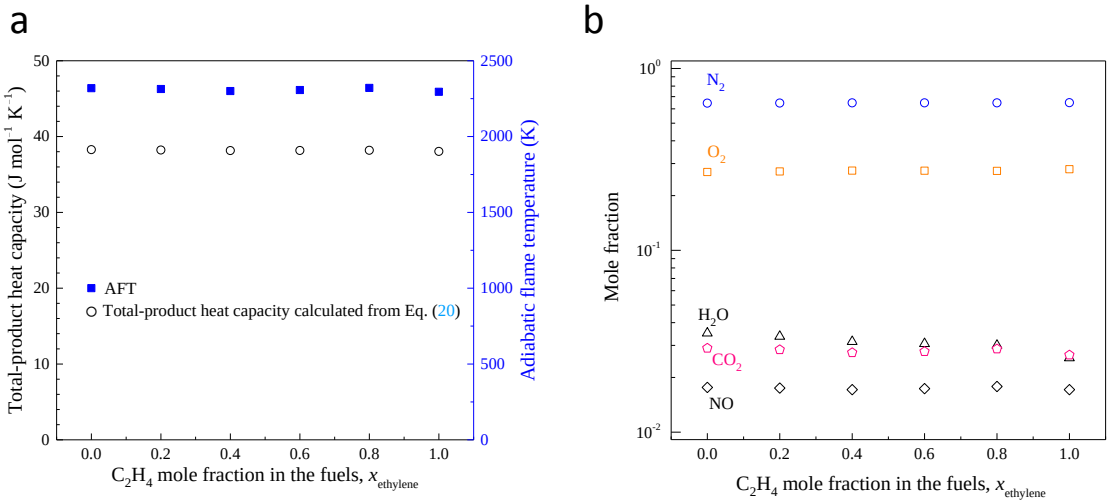

**Figure 7**

Figure 7

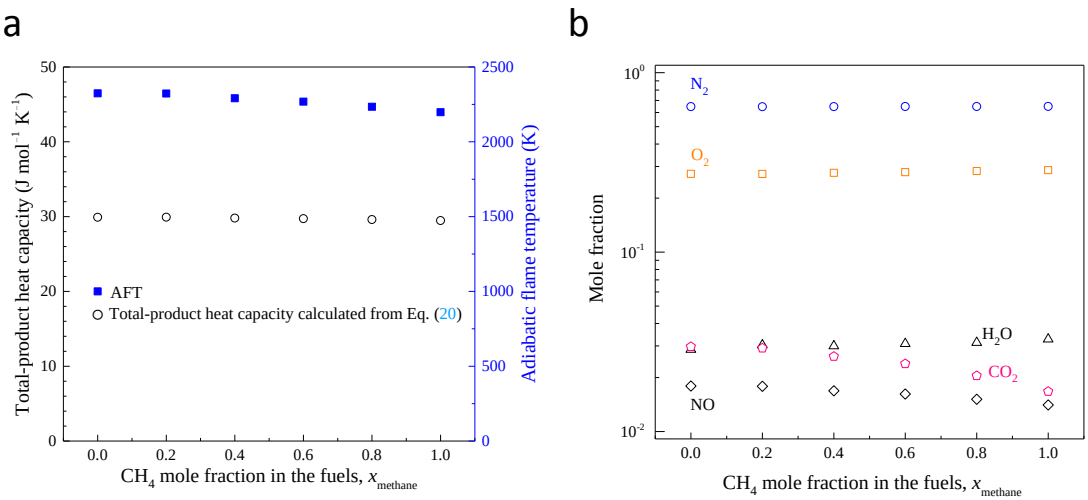

**Figure 8**

Figure 8

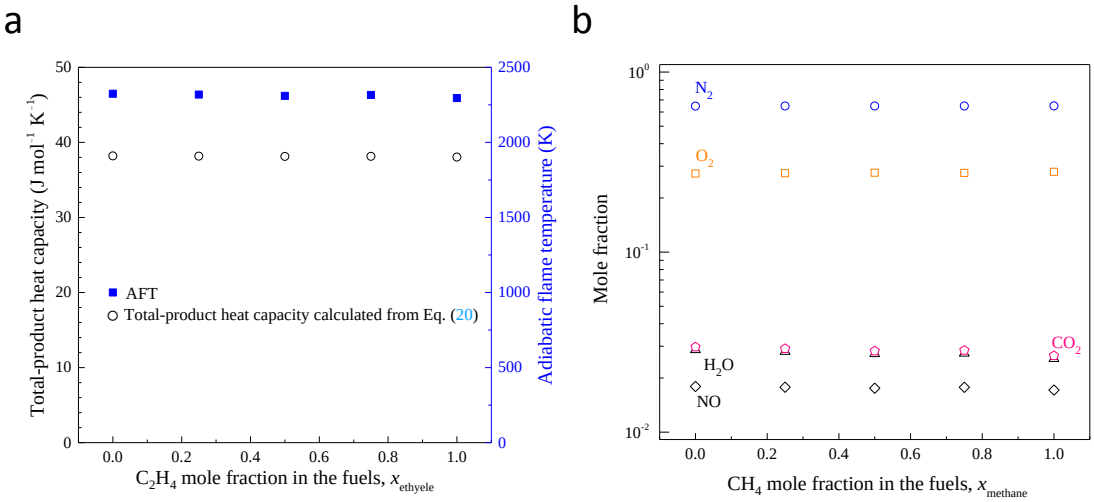

**Figure 9**

Figure 9

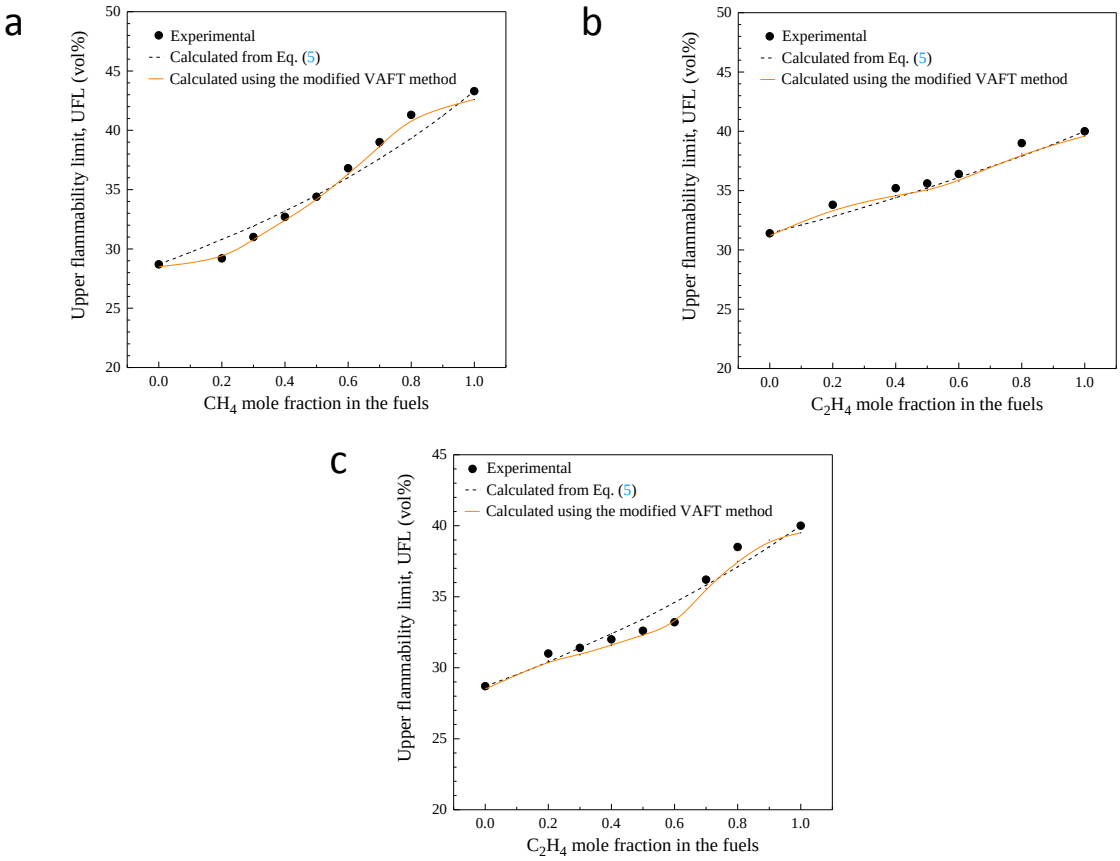

**Figure 10**

Figure 10

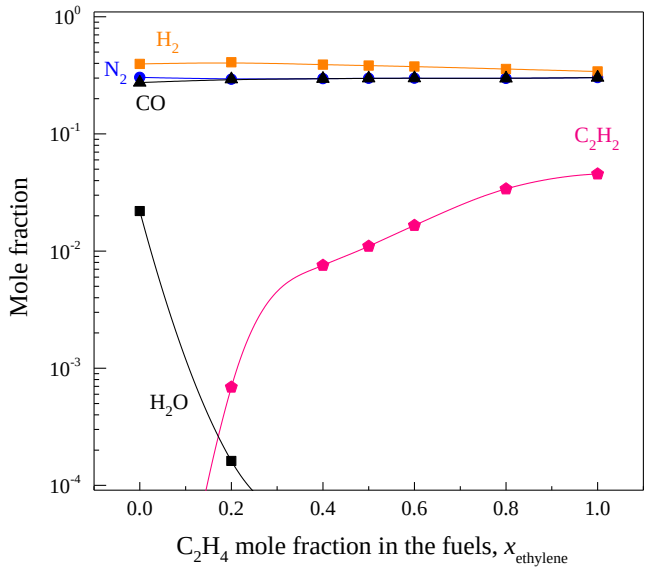

**Table 1**

Table 1

| | Flammable range (vol%) | | |
|---|---|---|---|
| | in $N_2O$ | in $O_2$ | in air |
| $C_2H_4$ | 2.0–40.0 [a] | 3.0–80 (Crowl and Louvar, 2011b) | 2.7–36 (Crowl and Louvar, 2011c) |
| | | | 3.1–32 (Chen, 2011) |
| | | | 2.6–27.4 (Schröder and Molnarne, 2005) |
| $C_3H_6$ | 1.5–28.7 [a] | 2.1–53 (Crowl and Louvar, 2011b) | 2.0–11 (Crowl and Louvar, 2011c) |

[a] Data were obtained from the present study.